Enhanced near-infrared QEPAS sensor for sub-ppm level H_2S detection by means of a fiber amplified 1582 nm DFB laser

Hongpeng Wu[1], Lei Dong[1,*], Huadan Zheng[1], Xiaoli Liu[1], Xukun Yin[1], Weiguang Ma[1], Lei Zhang[1], Wangbao Yin[1], Suotang Jia[1] and Frank K. Tittel[2]

[1)] *State Key Laboratory of Quantum Optics and Quantum Optics Devices, Institute of Laser Spectroscopy, Shanxi University, Taiyuan 030006, China*

[2)] *Department of Electrical and Computer Engineering, Rice University, Houston, TX 77004, USA*

Abstract: A power-boosted quartz-enhanced photoacoustic spectroscopy (QEPAS) sensor is developed for sub-ppm H_2S trace-gas detection in the near-infrared spectral region. The sensor is based on off-beam QEPAS with an erbium-doped fiber amplified 1582 nm distributed feedback (DFB) laser. The offset of the sensor floor noise caused by stray light and gas flow can be removed by an electrical modulation cancellation method, which lowers the noise to the theoretical thermal noise level. The sensor was optimized in terms of gas pressure and current modulation

* Corresponding author. Tel: +86 3517018904; fax: +86 3517018927.
E-mail address: donglei@sxu.edu.cn

depth for H_2S detection at 6320.6 cm^{-1}. The linearity of the sensor response to the laser power and H_2S concentration confirms that saturation does not occur. With ~ 1.4 W optical excitation power and 67 sec averaging time, a H_2S detection sensitivity of 142 ppbv (parts per billion by volume) is achieved at atmospheric pressure and room temperature, which is the best value, reported in the literature so far for H_2S QEPAS sensors. A side-by-side sensitivity comparison for different sensor systems is also reported.

Keywords: Trace gas detection; Quartz enhanced photoacoustic spectroscopy; Spectrophone; Erbium doped fiber amplifier; Modulation cancelation method

1. Introduction

Hydrogen sulfide (H_2S), one of the major air pollutants globally, is a colorless, toxic, flammable gas, which is mainly released into the atmosphere by burning of natural gas, fossil fuel, and other sulfur-bearing fuels as well as volcanic eruptions [1]. H_2S can also be found in well

water (occurs either naturally in well water or due to the presence of sulphate-reducing bacteria) and anywhere elemental sulfur is exposed to organic material [2] as well as sewers, swamps and waste treatment industries [3]. H_2S has an important impact on atmospheric chemistry as the product of the oxidation reaction with oxygen contributes to the formation of acid rain [4]. In the field of renewable energies, such as geothermal power plants, the monitoring of underground H_2S emission has significance in protecting people living in proximity of geothermal installations [5]. H_2S detection is also relevant in the field of clinical human breath analysis, because of its role as a biological signature of several pathological conditions [6]. Furthermore, H_2S even at low concentration levels is dangerous to human health. Long term exposure to concentrations below 150 parts per billion (ppb) by volume can cause headaches, irritability, conjunctiva congestion, poor memory and dizziness [1,6]. Hence, there is a need in developing reliable, cost-effective H_2S sensors, capable for detecting H_2S at sub-ppm (parts per million) concentration levels for applications in environmental monitoring, human pathologies research and industrial process control [7].

Photo-acoustic spectroscopy (PAS) is a traditional spectroscopic technique [4,7-10]. PAS has many attractive features, compared with other optical spectroscopic technique, such as relative simplicity, ruggedness and wavelength independence. Detection of H_2S concentration levels using PAS based optical gas sensor platforms were reported by numerous researchers. Szabó et al. [7] employed wavelength modulation, resonance frequency tracking and an easy-to-use method enabling in situ calibration to investigate H_2S detection, obtaining a detection sensitivity of 6 ppm when using a 1574.5 nm diode laser . Varga et al. [4] reported an H_2S detection limit of 0.5 ppm (3σ) with long averaging

times (~30 minutes) by means of PAS and a single-mode, fiber-coupled, telecommunication-type diode laser operating at 1574.5 nm. However, conventional microphone-based photo-acoustic cells are sensitive to environmental noise as their low resonance frequency values, typically < 2 kHz, and their sizes are considered to be large [11,12]. Quartz-enhanced photoacoustic spectroscopy (QEPAS), first reported in 2002, is a modification of conventional PAS, in which a commercially available piezoelectric quartz tuning fork (QTF) acts as an acoustic wave transducer to detect the sound signal generated by the trace gas absorbing the excitation laser beam [13]. The high resonant frequency f_0 (~32,768 Hz) and narrow resonance width (3–5 Hz) of the QTF improve QEPAS selectivity and immunity to environmental acoustic noise [14,15]. Recently some QEPAS-based H_2S sensors with different excitation laser sources have also been reported. Viciani et al. [5] and A. A. Kosterev et al. [16] studied the QEPAS-based H_2S sensors with a near-infrared distributed feedback (DFB) laser. Furthermore, the QEPAS sensor for H_2S by means of mid-infrared and THz laser sources were investigated by M. S. D. Cumis et al. [17] and V. Spagnolo et al. [18], respectively.

In all QEPAS-based H_2S sensors mentioned above, only the one employing the 7.9 μm mid-infrared laser as excitation light offers the capability of detecting H_2S at sub-ppm concentration levels in a few second integration time [17]. This is mainly due to the fact that fundamental bands in the mid-infrared region are at least one order of magnitude stronger than the transitions in near-infrared region [19]. However, near-infrared diode lasers can be attractive in trace gas detection, since they can be operated at room temperature with low cost, long life (> 10 years), low power consumption, and can be readily coupled to commercial optical fiber systems [3,20,21]. However, this approach is a big

challenge to achieve H_2S detection in the near infrared overtone absorption band region at sub-ppm concentration levels.

A distinct advantage of QEPAS is that the performance of QEPAS-based sensors can be improved as the excitation laser power is increased, since the QEPAS detection sensitivity scales linearly with excitation laser power. Optical fiber amplifiers, developed for the telecommunications industry to deliver optical signals over long distances, are commercially ready available, robust and low cost [22-25]. In an optical fiber amplifier, a short length of single-mode optical fiber, when doped with a small amount of an appropriate rare-earth ion, such as erbium, and then pumped with a ~ 980 nm semiconductor diode, can be used to achieve amplification factors of up to 3 orders of magnitude for input signals that occur within the gain bandwidth of the dopant [26]. Although amplification can theoretically be achieved over a wide range of wavelengths (0.651-2 μm), it is sufficiently mature enough only in three telecommunication bands (1450-1550 nm, 1520-1570 nm and 1565-1610 nm). Fortuitously, an ideal H_2S absorption line near 1.582 μm, free from H_2O and CO_2 interference, occurs in the erbium doped fiber amplifier (EDFA) operating band [22].

In this paper, we describe a QEPAS sensor combined with an EDFA for H_2S detection. Benefiting from the watt-level power output of an EDFA, the detection sensitivity of the QEPAS based sensor using a near infrared laser source is considerably improved. Performance of power-boosted quartz-enhanced photo-acoustic spectroscopy is investigated and optimized.

2. Description of experimental system

A schematic of the power-boosted QEPAS sensor for H_2S detection is depicted in Fig. 1. A near-infrared distributed feedback (DFB) diode laser (FITEL Inc. Model FRL15DCWD-A82) with a center wavelength of 1582.1 nm served as the excitation source. The DFB laser was mounted onto a driver board which was connected to a computer via a RS232 serial port. Hence the DFB laser temperature and current can be controlled by means of computer. The DFB laser beam was directed to an EDFA (Connect Laser Technology Ltd. Model MFAS-L-EY-B-MP) by means of an optical fiber. The EDFA offers an adjustable output power from 30 mW to 1500 mW with the same wavelength as the seed laser. An opto-isolator (Connect Laser Technology Ltd. Model A12104132) was utilized to protect the DFB laser against back reflections. The output laser beam from the opto-isolator was focused into a 100 μm-diameter light spot by a fiber-coupled focuser (OZ optics Ltd. Model LPF-01) with 10 mm focal length, and an acoustic detection module (ADM) was placed at the focal point of the focuser. As a result, the laser beam passed without touching any surfaces. The ADM for the power-boosted QEPAS sensor incorporates a QTF and an acoustic micro-resonator (AmR) that leads to a further enhancement of the QEPAS signal. AmRs are usually in either an “on beam” or “off beam” configuration. In the “on beam” configuration, two identical metallic thin tubes are placed along the excitation laser beam and close to QTF with a 20-50 μm gap [14,27,28]. Optimum “on beam” QEPAS yields a signal-to-noise ratio (SNR) gains of ~30 times than the original bare QTF based QEPAS geometry [29]. However, very careful active optical alignment is required for the “on beam” scheme as the gap between the QTF prongs is only 0.2-0.3 mm

wide and the total length of the AmR beam path is ~8-10 mm [14]. Therefore, the "on beam" scheme is not used for power-boosted QEPAS sensors. Instead, as shown in Fig. 1, the "off beam" configuration was employed. The excitation laser beam was coupled through the AmR, while the QTF was placed external to the AmR and "listened" to the photo-acoustic signal via a small slit made in the middle of the AmR. This "off beam" configuration can optimally avoid touching the QTF by the laser excitation beam. Although the "off beam" configuration has a weaker SNR gain in contrast to the "on beam" configuration, the high power employed can easily compensate for the loss. A thin metal tube of 5.84 mm in length with a 0.8 mm inner diameter and a 1.24 mm outer diameter was chosen as the AmR. The QTF was placed as close as possible to, but not touching, the slit (~0.65 mm in length and ~0.15 mm in width). All the geometrical parameters of the tube are optimal for "off beam" QEPAS as reported in Refs. [30-32].

The ADM was enclosed inside a gas enclosure with two antireflection coated CaF_2 windows. A gas mixing and sampling system, consisted of two mass flow controllers (MFCs) (Beijing Seven star Electronics Co. Model D07-12A, D07-19B) and two gas cylinders were constructed and located upstream to generate a H_2S / N_2 gas mixture of a fixed concentration. A pressure controller (MKS Instruments Inc. Model 649B13TS1M22M) and a vacuum pump (Oerlikon Leybold Vacuum Inc. Model D16C) were placed downstream to control and maintain the power-boosted QEPAS sensor system pressure. The flow rate was set at a constant rate of 100 sccm.

A 2*f* wavelength-modulation spectroscopy (2*f* -WMS) approach was implemented by applying a sine wave to the driver board to modulate

the laser wavelength [33]. The sine wave was supplied by function generator 1(Agilent Model 33210A) and its frequency was set to one half of the QTF resonant frequency ($f = f_0/2$). When the QTF-generated current signal was detected, the signal output from one electrode of the QTF was directed to a custom made transimpedance amplifier with a feedback resistor of R_g=10 MΩ to convert the current signal into a voltage signal, and directed to a lock-in amplifier (Stanford Research Systems, Model SR830) for demodulation in the 2*f* mode. Meanwhile, the other electrode was connected to ground (the switch I in Fig. 1 was set to position 1 and the function generator 2 was disabled). For all measurements reported in this paper, the lock-in amplifier was set to a 12 dB/oct filter slope and a time constant, τ=300 ms. All of the data acquisition and processing for this power-boosted QEPAS sensor was controlled by a computer based Labview program.

3. Effect of high power laser excitation

3.1 Analysis of saturation effect

Generally, the QEPAS signal can be expressed as [34]:

$$S = C_{\mathrm{ADM}} P_0 C \alpha(p) \varepsilon(p) Q(p) \qquad (1)$$

where C_{ADM} is the ADM constant, P_0 is the power of the incident laser radiation, p is the gas pressure, $\alpha(p)$ is the peak intensity of the 2*f* absorption spectrum, $\varepsilon(p)$ is the conversion efficiency and $Q(p)$ is the quality factor of the acoustic resonator. However, at high excitation optical power, Eq. (1) may be no longer valid and a saturation effect has to be taken into account [35-37]. The absorption of the incident light causes gas

molecules to be excited to higher energy levels which then decay via spontaneous emission or collisional de-excitation [38,39]. When the laser power is low, the molecular number densities N of the lower state can maintain this process. Meanwhile, the relationship of the upper state molecules number densities N_u and the total molecules number densities N can be expressed by the following expression [40]:

$$\frac{N_u}{N} = \frac{(\frac{I}{h\upsilon})(\frac{S_{line}}{\pi\Delta\nu})}{2(\frac{I}{h\upsilon})(\frac{S_{line}}{\pi\Delta\nu}) + \tau_0^{-1} + \tau_1^{-1}} \quad (2)$$

where I is the light intensity, S_{line} is the absorption line strengths, ν is the frequency of the incident laser, $\Delta\nu$ is line width of the transition, τ_0 and τ_1 are non-radiation relaxation time and radiation relaxation time, respectively. When the laser intensity is sufficiently high, the following condition will be met:

$$2(\frac{I}{h\upsilon})(\frac{S_{line}}{\pi\Delta\nu}) \gg (\tau_0^{-1} + \tau_1^{-1}) \quad (3)$$

and Eq. (2) is simplified to a constant:

$$\frac{N_u}{N} = \frac{1}{2} \quad (4)$$

That implies that the depletion from the vibrational excited level slows in comparison with the pump rate due to the high laser power. There are no more molecules to be excited to higher energy levels with increasing laser power. In other words, the transition is saturated. The QEPAS signal will not benefit from further higher laser excitation power.

In order to avoid the nonlinear response of the sensor from the saturation effect, an experiment to check the saturation level was carried out. A certified mixture of 50 ppmv H_2S in nitrogen (N_2) was used. Several 2*f*-QEPAS spectral scan acquisitions with an optimal modulation depth of 20 mA were obtained for different laser powers at atmospheric pressure (p=760 Torr) and room temperature (T_{room}=297.2 K).

The actual output powers from the EDFA were varied from 100 mW to 1,500 mW which corresponds to 80.6 mW to 1,402 mW displayed on a power meter (Ophir Optronics Solutions Ltd. Model 660745) behind the QEPAS spectrophone, due to transmission losses from the CaF_2 windows and the ADM. The laser power monitored behind the QEPAS spectrophone was used to analyze the experimental results.

The measured QEPAS peak values with the different powers are reported in Fig. 2. A linear fitting routine was implemented. The obtained R square value of 0.999 proves the linear response of the sensor to laser power and confirms that the sensor had not reached the saturation condition [37]. In this case, further evaluation tests were performed at an incident laser power of 1,402 mw in order to obtain the highest QEPAS signal.

3.2 Background noise analysis and elimination

The background noise must be analyzed, as the detection sensitivity of a trace gas sensor is determined by the SNR. For a traditional QEPAS sensor a laser source with low power and good beam quality can be used, as verified in several experimental studies that showed that the observed QEPAS noise is equal to the thermal noise of the QTF and the feedback resistor [41-44]. The thermal noise can be expressed as:

$$\sqrt{V_{N-R}^2}+\sqrt{V_{N-R_g}^2}=\frac{R_g}{\sqrt{2}}\sqrt{\frac{4k_BT\Delta f}{R}}+\frac{\sqrt{4k_BTR_g\Delta f}}{\sqrt{2}} \quad (5)$$

$$R=\frac{1}{Q}\sqrt{\frac{L}{C}} \quad (6)$$

where R_g=10 MΩ is the amplifier feedback resistor, k_B is the Boltzmann constant, Δf is the detection bandwidth, T is QTF temperature, and R, L and C are the electrical parameters of the QTF when represented by an equivalent series resonant circuit. The QTF-related parameters can be obtained by analyzing the QTF response profile as a function of excitation frequency. The response profile was obtained by applying a sine wave excitation voltage from function generator 2(Agilent Model 33210A) to the QTF electrode which is connected to ground when the QEPAS signal is detected. Specifically, in this mode, the switch Ⅰ in Fig. 1 was set to position 2, switch Ⅱ was disconnected and the attenuator was disabled. When the frequency of the excitation signal was scanned, the lock-in amplifier was set to the 1f mode to demodulate the piezoelectric signal produced by the excited vibration, and the time constant was set at 300 ms. A theoretical thermal noise of 2.23 μV was obtained with measured parameters of the QTF (f_0=32757.86 Hz, Q=9, 064 and R=278.5 kΩ).

Subsequently, the virtual noise of the power-boosted QEPAS based H_2S sensor was measured via a 2f WMS approach. The diode laser wavelength with an output power of 1, 402 mW was set to target a H_2S absorption line at 6320.6 cm^{-1}. The gas enclosure was first filled with pure N_2 at atmospheric pressure and room temperature. An offset floor of ~39.02 μV was observed which is ~17 times higher than the theoretical

thermal noise value, as shown in Fig. 3. This offset floor is partly caused by the stray light from beam quality of the EDFA laser output. This stray light leads to periodical heating of the QTF surface [40]. The absorption of the CaF_2 windows and the ADM is another reason. This offset floor is a side effect when using a watt level laser [32] because there are no experiments that exhibit an offset floor for diode lasers emitting several tens of milliwatts [30,32]. An additional offset of ~6 μV was observed when the N_2 flow was 100 sccm, so that the total offset floor was ~20 times larger than the QEPAS thermal noise level.

In order to minimize or eliminate the higher offset floor, an electrical modulation cancellation method (E-MOCAM) was used as shown in the dotted box in Fig. 1. The basic concept of this method is to electrically induce the QTF vibrating with an opposite phase with regard to the vibration caused by stray light and gas flow, so that the offset floor is cancelled [41,45,46]. To implement E-MOCAM, the switch Ⅰ in Fig. 1 was set to position 2, and the switch Ⅱ was switched on. A sine wave supplied by function generator 2 was sent to the QTF electrode. This sine wave has the same frequency as the QTF resonant frequency f_0, but the opposite phase. The correct phase relationship was ensured by the trigger from function generator 1 to function generator 2. In this case, the amplitude and phase of the two sine waves can be adjusted independently. In addition, an electrical attenuator was utilized to provide amplitude tuning at the microvolt level for the balancing signal, as shown in Fig. 1. The virtual noise was measured again after the E-MOCAM was activated. The 1σ value of the noise was now 2.52 μV which is in agreement with the thermal noise.

4. Optimization and performance of power-boosted QEPAS sensor for H_2S detection

In Eq. (1), α depends on the laser wavelength modulation depth and α, ε and Q are all pressure dependent. Hence, in order to optimize the sensor performance, both the gas pressure and laser wavelength modulation depth must be chosen appropriately [47,48]. The optimization was carried out with a 50 ppmv H_2S in N_2 mixture. The detection was based on 2*f* WMS approach by dithering and scanning the laser current, as described in section 2. The phase and amplitude of the sine wave that is used to balance the background noise were adjusted carefully every time the gas mixing pressure was changed. A H_2S absorption line at 6320.6 cm^{-1} was chosen as the target line as mentioned previously in section 3.2. An example of the 2*f* signal of 50 ppm H_2S acquired at 300 Torr and 760 Torr is shown in Fig. 4a. The peak absorption of the H_2S power-boosted QEPAS 2*f* signal was depicted in Fig. 4b as a function of the gas mixing pressure and laser current modulation depth. At higher pressure the target line merges with its weaker neighbor at 6320.5 cm^{-1} and 6320.9 cm^{-1}. This explains why the signals for lower pressure ($P \leq 300$ Torr) show different changing characteristics with respect to the signals for higher pressure ($P \geq 400$ Torr).

A maximum QEPAS signal was observed at 400 Torr and with a current modulation depth of ~15 mA. In fact, the power-boosted QEPAS signal value with 20 mA current modulation depth at the pressure of 760 Torr is only ~8% lower than the maximum H_2S signal. It is more convenient to operate the power-boosted QEPAS sensor at atmospheric pressure with only a slightly higher modulation depth because in this case the sensor system can be simplified by removing both the pressure controller and flow meter. Hence, further evaluation tests of the

power-boosted QEPAS based H_2S sensor were performed at atmospheric pressure with a 20 mA current modulation depth. Based on the measured noise level and the data depicted in Fig. 4b, a 1σ minimum detectable concentration limit of 734 ppb was obtained at 1 s data acquisition time and 1,402 mw laser power. The time constant of lock-in amplifier was 300 ms corresponding to a detection bandwidth of Δf =0.833 Hz. Hence the corresponding normalized noise equivalent absorption (NNEA) coefficient for H_2S is 9.8×10^{-9} W·cm^{-1}/√Hz.

The linearity of the power-boosted QEPAS based H_2S sensor was evaluated by measuring its response to the different H_2S concentrations from 0 to 50 ppm. The data acquisition time was set to 1 sec and the results of repetitive measurements are plotted in Fig. 5a. Data for each step are averaged and plotted against the H_2S concentrations in Fig. 5b. The results confirm the linearity of this sensor response to the H_2S concentration.

To evaluate the long term stability of such a power-boosted QEPAS sensor an Allen-Werle deviation analysis was performed. The ADM was filled with pure N_2 at atmospheric pressure and room temperature, and the laser frequency was locked to the H_2S absorption line at 6320.6 cm^{-1}. The result of this analysis is shown in Fig. 6. The Allan-Werle deviation follows a 1/√t dependence for time sequences ranging from 1 to 67 s, which indicates that white noise of the QTF remains the dominant noise source. Mainly limited by the stability of the EDFA, the Allan-Werle deviation experiences a sensitivity drift following a √t dependence when the averaging time exceeds 100 s. Thus the optimal detection sensitivity can be reduced to 142 ppb for a 67 s integration time.

Laser sources at three different spectral regions have been used as the exciting radiation in QEPAS-based sensors for H_2S detection benefiting from the wavelength independence of the QEPAS based trace gas sensor. A side-by-side comparison for the three different QEPAS based sensors is shown in Table 1. With the same excitation wavelength of 6320.6 cm^{-1} in Ref [16] and our work, the detection limit was not proportional to the excitation laser power as expected from Eq. (1). The reason for this discrepancy is due to the different configurations of the two sensor architectures. The sensitivity enhancement factor for the off-beam configuration is lower than that of the on-beam design. However, the highest sensitivity was obtained with the reported power-boosted QEPAS-based sensor. In fact, the higher excitation laser power compensates for the smaller enhancement factor provided by the off-beam QEPAS sensor configuration as well as the weaker absorption line strength compared with the absorption lines in the mid-IR or THz spectral regions.

5. Conclusions

In summary, a power-boosted QEPAS-based H_2S sensor system was developed using an EDFA and a 1582 nm DFB laser. E-MOCAM was employed to remove the offset noise floor of the zero QEPAS signal. The first demonstration of the use of an EDFA enhancing QEPAS-based sensor detection scheme in the near infrared is reported. With a laser power of 1.4 W, the sensor achieved a fast (1 s integration time) H_2S detection sensitivity of 734 ppb at atmospheric pressure and room temperature. The detection limit can be further decreased to 142 ppb with an integration time of ~67 s. Our reported QEPAS sensor system obtained the lowest H_2S detection limit compared with other H_2S QEPAS

platforms reported in the literature. The influence of water vapor on the measurement results was not investigated in this study. Water can affect the QEPAS signal amplitude by acting as a promoter of vibrational-translational relaxation process based on the Ref. [5] and [16]. This effect is also valid at high excitation optical power. Further improvement of the detection sensitivity should be feasible for an on-beam ADM configuration by improving the beam quality of the high power laser output from an EDFA by means of a more efficient optical beam collimator. Furthermore the offset noise floor can also be removed by employing a custom QTF with a larger gap size between two prongs, which will simplify the sensor configuration and offer a more rugged and stable QEPAS sensor performance.

Acknowledgments

The work was supported by National Natural Science Foundation of China (Grant #s. 61275213, 61108030, 61475093, 61127017, 61178009, 61378047 and 61205216), the National Key Technology R&D Program (2013BAC14B01), the Shanxi Natural Science Foundation (2013021004-1), and the Shanxi Scholarship Council of China (2013-011, 2013-01). Frank K Tittel acknowledges support by the National Science Foundation (NSF) ERC MIRTHE award and the Robert Welch Foundation (Grant C-0586).

References

[1] W. Chen, A. A. Kosterev, F. K. Tittel, X. Gao, W. Zhao, H_2S trace concentration measurements using off-axis integrated cavity output spectroscopy in the near-infrared, Appl. Phys. B 90 (2008) 311–315.

[2] L. L. Barton, G. D. Fauque, Physiology and biotechnology of sulfate-reducing bacteria, Adv. in Appl. Microbiol. 68 (2009) 41-98.

[3] G. Modugno, C. Corsi, M. Gabrysch, M. Inguscio, Detection of H_2S at the ppm level using a telecommunication diode laser, Opt. Commun. 145 (1998) 76-80.

[4] A. Varga, Z. Boz´oki, M. Szak´all, G. Szab´o, Photoacoustic system for on-line process monitoring of hydrogen sulfide (H_2S) concentration in natural gas streams, Appl. Phys. B 85 (2006) 315-321.

[5] S. Viciani, M. S. de Cumis, S. Borri, P. Patimisco, A. Sampaolo, G. Scamarcio, P. D. Natale, F. D'. Amato, V. Spagnolo, A quartz-enhanced photoacoustic sensor for H_2S trace-gas detection at 2.6 μm, Appl. Phys. B 119 (2015) 21-27.

[6] L. Ciaffoni, R. Peverall, G. A. D. Ritchie, Laser spectroscopy on volatile sulfur compounds: possibilities for breath analysis, J. Breath Res. 5 (2011) 024002.

[7] A. Szabo´, A´. Moha´csi, G. Gulya´s, Z. Bozo´ki, G. Szabo´, In situ and wide range quantification of hydrogen sulfide in industrial gases by means of photoacoustic spectroscopy, Meas. Sci. Technol. 24 (2013) 065501.

[8] M. Köhring, S. Böttger, U. Willer, W. Schade, Temperature effects in tuning fork enhanced interferometric photoacoustic spectroscopy, Opt. Express 21 (2013) 20911-20922.

[9] T. Laurila, H. Cattaneo, V. Koskinen, J. Kauppinen, R. Hernberg, Diode laser-based photoacoustic spectroscopy with interferometrically-enhanced cantilever detection, Opt. Express 13 (2005) 2453-2458.

[10] Y. Cao, W. Jin, L. Ho, and Z. Liu, Evanescent-wave photoacoustic spectroscopy with optical micro/nano fibers, Opt. Lett. 37 (2012) 214-216.

[11] N. Petra, J. Zweck, A. A. Kosterev, S. E. Minkoff, D. Thomazy, Theoretical analysis of a quartz-enhanced photoacoustic spectroscopy sensor, Appl. Phys. B 94 (2009) 673-680.

[12] L. Dong, V. Spagnolo, R. Lewicki, F. K. Tittel, Ppb-level detection of nitric oxide using an external cavity quantum cascade laser based QEPAS sensor, Opt. Express 19 (2011) 24037-24045.

[13] A. A. Kosterev, Y. A. Bakhirkin, R. F. Curl, F. K. Tittel, Quartz-enhanced photoacoustic spectroscopy, Opt. Lett. 27 (2002) 1902–1904.

[14] L. Dong, A. A. Kosterev, D. Thonazy, F. K. Tittel, QEPAS spectrophones: design, optimization, and performance, Appl. Phys. B 100 (2010) 627-635.

[15] M. Köhring, A. Pohlkötter, U. Willer, M. Angelmahr, W. Schade, Tuning fork enhanced interferometric photoacoustic spectroscopy: a new method for trace gas analysis, Appl. Phys. B 102 (2011) 133-139.

[16] A. A. Kosterev, L. Dong, D. Thomazy, F. K. Tittel, S. Overby, QEPAS for chemical analysis of multi-component gas mixtures, Appl. Phys. B 101 (2010) 649–659.

[17] M. S. D. Cumis, S. Viciani, S. Borri, P. Patimisco, A. Sampaolo, G. Scamarcio, P. D. Natale, F. D'Amato, V. Spagnolo, Widely-tunable mid-infrared fiber-coupled quartz-enhanced photoacoustic sensor for environmental monitoring, Opt. Express 22 (2014) 28222-28231.

[18] V. Spagnolo, P. Patimisco, R. Pennetta, A. Sampaolo, G. Scamarcio, M. S. Vitiello, F. K. Tittel, THz Quartz-enhanced photoacoustic sensors for H_2S trace gas detection, Opt. Express 23 (2015) 7574-7582.

[19] The HITRAN database can be found at: http://www.hitran.com

[20] A. D. Bykov, O. V. Naumenko, M. A. Smirnov, L. N. Sinitsa, L. R. Brown, J. Crisp, D. Crisp, The Infrared Spectrum of H_2S from 1 to 5 μm, Can. J. Phys. 72 (1994) 989-999.

[21] J. M. Flaud, R. Grosskloss, S. B. Rai, R. Stuber, W. Demtroder, D. A. Tate, L. G. Wang, T. F. Gallagher, Diode Laser Spectroscopy of $H_2{}^{34}S$ Around 0.82 μm, J. Mol. Spectrosc. 172 (1995) 275-281.

[22] P. W. France, Optical fiber lasers and amplifiers, CRC Press (1991).

[23] D. Richter, D. G. Lancaster, F. K. Tittel, Development of an automated diode-laser-based multicomponent gas sensor, Appl. Opt. 39 (2000) 4444–4450.

[24] D. Richter, A. Fried, B. P. Wert, J. G. Walega, F. K. Tittel, Development of a tunable mid-IR difference-frequency laser source for highly-sensitive airborne trace gas detection, Appl. Phys. B 75 (2002) 281–288.

[25] P. M. Becker, A. A. Olsson, J. R. Simpson, Erbium-doped fiber amplifiers: fundamentals and technology, Academic Press (1999).

[26] M. E. Webber, M. Pushkarsky, C. K. N. Patel, Fiber-amplifier-enhanced photoacoustic spectroscopy with near-infrared tunable diode lasers, Appl. Opt. 42 (2003) 2119-2126.

[27] L. Dong, H. Wu, H. Zheng, Y. Liu, X. Liu, W. Jiang, L. Zhang, W. Ma, W. Ren, W. Yin, S. Jia, F. K. Tittel, Double acoustic micro-resonator quartz enhanced photoacoustic spectroscopy, Opt. Lett. 39 (2014) 2479-2482.

[28] H. Wu, L. Dong, W. Ren, W. Yin, W. Ma, L. Zhang, S. Jia, F. K. Tittel, Position effects of acoustic micro-resonator in quartz enhanced photoacoustic spectroscopy, Sens. Actuators B: Chem. 206 (2015) 364–370.

[29] H. Yi, W. Chen, S. Sun, K. Liu, T. Tan, X. Gao, T-shape microresonator-based high sensitivity quartz-enhanced photoacoustic spectroscopy sensor, Opt. Express 20 (2012) 9187-9196.

[30] K. Liu, X. Guo, H. Yi, W. Chen, W. Zhang, X. Gao, Off-beam quartz-enhanced photoacoustic spectroscopy, Opt. Lett. 34 (2009) 1594–1596.

[31] K. Liu, H. Yi, A. A. Kosterev, W. Chen, L. Dong, L. Wang, T. Tan, W. J. Zhang, F. K. Tittel, X. Gao, Trace gas detection based on off-beam quartz enhanced photoacoustic spectroscopy: optimization and performance evaluation, Rev. Sci. Instrum. 81 (2010) 103103.

[32] H. Yi, K. Liu, W. Chen, T. Tan, L. Wang, X. Gao, Application of a broadband blue laser diode to trace NO_2 detection using off-beam quartz enhanced photoa-coustic spectroscopy, Opt. Lett. 36 (2011) 481–483.

[33] V. Spagnolo, A. A. Kosterev, L. Dong, R. Lewicki, F. K. Tittel, NO trace gas sensor based on quartz-enhanced photoacoustic spectroscopy and external cavity quantum cascade laser, Appl. Phys B 100 (2010) 125–130.

[34] A. A. Kosterev, Y. A. Bakhirkin, F. K. Tittel, S. Mcwhorter, B. Ashcraft, QEPAS methane sensor performance for humidified gases, Appl. Phys B 92 (2008) 103-109.

[35] Y. Yuan, Z. Yan, G. Meng, Z. Li, L. Shang, Photoacoustic signal saturation characteristics of concentrated gases, Acta. Phys. Sin. 59 (2010) 6908-6913.

[36] F. J. M. Harren, F. G. C. Bijnen, J. Reuss, L. A. C. J. Voesenek, C. W. P. M. Blom, Sensitive intracavity photoacoustic measurements with a CO_2 waveguide laser, Appl. Phys B 50 (1990) 137-144.

[37] D. C. Dumitras, D. C. Dutu, C. Matei, A. M. Magureanu, M. Petrus and C. Popa, Laser photoacoustic spectroscopy: principles, instrumentation, and characterization, J. Optoelectron. Adv. Mater. 9 (2007) 3655–3701.

[38] J. W. Daily, Saturation effects in laser induced fluorescence spectroscopy, Appl. Opt. 16 (1977) 568-571.

[39] N. Tsukada, Y. Murakami, T. Ogawa, Saturation effects of transverse resonances in optical pumping experiments, J. Phys. B: Atom. Molec. Phys. 6 (1973) 2650-2612.

[40] Q. Yin, T. Wang, M. Qian, Optothermal spectroscopy technique and its application, Science Press (1999).

[41] H. Zheng, L. Dong, X. Yin, X. Liu, H. Wu, L. Zhang, W. Ma, W. Yin, S. Jia, Ppb-level QEPAS NO_2 sensor by use of electrical modulation cancellation method with a high power blue LED, Sens. Actuators B: Chem. 208 (2015) 173–179.

[42] A. A. Kosterev, F. K. Tittel, Ammonia detection by use of quartz-enhanced photoacoustic spectroscopy with a near-IR telecommunication diode laser, Appl. Opt. 43 (2004) 6213-6217.

[43] A. A. Kosterev, P. R. Buerki, L. Dong, M. Reed, T. Day, F. K. Tittel, QEPAS detector for rapid spectral measurements, Appl. Phys. B 100 (2010) 173-180.

[44] A. A. Kosterev, F. K. Tittel1, D. V. Serebryakov, A. L. Malinovsky, I. V. Morozov, Applications of quartz tuning forks in spectroscopic gas sensing, Rev. Sci. Instrum. 76 (2005) 043105.

[45] V. Spagnolo, L. Dong, A. A. Kosterev, D. Thomazy, J. H. Doty III, F. K. Tittel, Modulation cancellation method for measurements of small temperature differences in a gas, Opt. Lett. 36 (2011) 460–462.

[46] V. Spagnolo, L. Dong, A. A. Kosterev, D. Thomazy, J. H. Doty III, F. K. Tittel, Modulation cancellation method in laser spectroscopy, Appl. Phys. B 103 (2011) 735-742.

[47] Y. Ma, R. Lewicki, M. Razeghi, F. K. Tittel, QEPAS based ppb-level detection of CO and N_2O using a high power CW DFB-QCL, Opt. Expr. 21 (2013) 1008-1019.

[48] S. Schilt, L. Thevenaz, P. Robert, Wavelength modulation spectroscopy: combined frequency and intensity laser modulation, Appl. Opt. 42 (2003) 6728-6738.

Figure captions

Fig. 1 Schematic of the power-boosted QEPAS sensor. MFC: mass flow controllers;

NV: needle valve; V: valve; ADM: acoustic detection module.

Fig. 2 Power-boosted QEPAS signal as a function of the actual power measured after the spectrophone.

Fig. 3 Noise analysis of the power-boosted QEPAS based H_2S sensor. The squares, circles and triangles showed the background noise caused by stray light and gas flow (100 sccm), background noise caused by stray light (0 sccm) and the final noise after activating E-MOCAM, respectively.

Fig.4 a. Power-boosted QEPAS spectra of the same H_2S absorption lines acquired at 300 Torr and 760 Torr, respectively. b. Power-boosted QEPAS signal corresponding to the peak H_2S absorption near 6320.6 cm^{-1} for different gas pressures and laser current modulation depths. All measurements were performed with a 50 ppmv H_2S in N_2 mixture and a 300 ms lock-in amplifier time constant.

Fig. 5 a. Power-boosted QEPAS signal repetitively recorded as a function of time for H_2S concentration values ranging from 1ppm to 50 ppm. b. Same data averaged and plotted as a function of H_2S concentration

Fig. 6 Allan-Werle deviation as a function of the data averaging period. Solid circles trace: laser frequency was locked to the H_2S absorption line at 6320.6 cm^{-1}, data acquisition time 1 s. Dotted line: $1/\sqrt{t}$ slope. Dashed line: $\sqrt{t}$ slope.

Table

Table 1 Intercomparison of QEPAS based sensors for H_2S detection operating in different spectral ranges.

	Near-IR		Near-IR	Mid-IR	THz
	this paper	[16]	[5]	[17]	[18]
ADM configuration	Off-beam	On-beam	On-beam	On-beam	Bare QTF
Frequency, cm^{-1}	6320.6	6320.6	3788.56	1266.93	97.11
Laser power, mW	1402	38.3	3	45	0.24
Linestrength, cm/mol	1.11×10^{-22}	1.11×10^{-22}	1.67×10^{-21}	1.51×10^{-21}	1.13×10^{-22}
Detection limit	734 ppt	10.1 ppm	4 ppm	1.3 ppm	Not available
NNEA, $W\cdot cm^{-1}/\sqrt{Hz}$	9.8×10^{-9}	5.8×10^{-9}	2.4×10^{-9}	2.1×10^{-8}	4.4×10^{-10}
Detection limit for longer integration time	142 ppb @67 s	Not available	500 ppb @60 s	330 ppb @30 s	13 ppm @30 s

Biographies:

Hongpeng Wu received his B.S. degree in physics from Shanxi University, China, in 2011. He is now pursuing a Ph.D. degree of atomic and molecular physics from the Institute of Laser Spectroscopy at Shanxi University. His research interests include gas sensors, photoacoustic spectroscopy, and laser spectroscopy techniques.

Lei Dong received his Ph.D. degree in optics from Shanxi University, China, in 2007. From June, 2008 to December, 2011, he worked as a post-doctoral fellow in the Electrical and Computer Engineering Department and Rice Quantum Institute, Rice University, Houston, USA. Currently he is a professor in the Institute of Laser Spectroscopy of Shanxi University. His research interests include optical sensors, trace gas detection, and laser spectroscopy.

Huadan Zheng received his B.S. degree in physics from Shanxi University, China, in2012. He is now pursuing a Ph.D. degree of atomic and molecular physics from the Institute of Laser Spectroscopy at Shanxi University. His research interests include gas sensors, photoacoustic spectroscopy, and laser spectroscopy techniques.

Xiaoli Liu received her B.S. degree in physics from Shanxi University, China, in 2013. She is now pursuing the M.S. degree of optics from the Institute of Laser Spectroscopy at Shanxi University. Her research interests include photoacoustic spectroscopy and laser spectroscopy

techniques.

Xukun Yin received his B.S. degree in physics from Shanxi University, China, in2014. He is now pursuing the M.S. degree of optics from the Institute of Laser Spectroscopy at Shanxi University. His research interests include gas sensors and laser spectroscopy techniques.

Weiguang Ma received his Ph.D. degree in optics from Shanxi University, China, in 2005. From April, 2006 to January, 2009, he worked as a post-doctoral fellow in the Department of Physics of Umeå University, Sweden. Now he is an associate professor of Shanxi University. His research interests include optical parameter oscillation, sum frequency generation, highly sensitive laser spectroscopy, and trace gas detection.

Lei Zhang received his Ph.D. degree in atomic and molecular physics from Shanxi University, China, in 2008. Now he is an associate professor of Shanxi University. His research interests include laser-induced breakdown spectroscopy and precision laser spectroscopy.

Wangbao Yin received his B.S. degree in physics from Shanxi University, China, in 1986, and a PhD degree in the Laser Spectroscopy Laboratory from Shanxi University, China, in 2003. He is currently a professor in the Institute of Laser Spectroscopy of Shanxi University. His research interests are environmental sensors, flexible electronic packaging, and application of laser spectroscopy.

Suotang Jia received his B.S. degree in physics in 1986 and the M.S. degree in optics in 1989 from Shanxi University, China. He graduated in 1994 with a Ph.D. degree for research in laser spectroscopy from the East China Normal University. Since 1996, he has worked as a visiting scholar at CNRS in France, the University of Maryland, Yale University, and University of Connecticut. He is now a professor at Shanxi

University and became President of Shanxi University in 2012. His research interests include quantum optics, quantum information, ultracold atom and molecular, and application of laser spectroscopy.

Frank K. Tittel received his B.S. degree in 1955 and the Ph.D. degree in 1959 from Oxford University. Now he is the J. S. Abercrombie Professor in the School of Engineering, Rice University, Houston, USA. Professor Frank Tittel has been involved in many innovative developments in quantum electronics and laser technology since the discovery of the laser in 1960, with applications ranging from laser spectroscopy to environmental monitoring. The most recent designs utilize novel quantum cascade and interband cascade lasers to achieve compact, robust instrumentation that can be deployed for field applications, such as at NASA's Johnson Space Center related to air and water quality issues relevant to the International Space Station, for urban formaldehyde monitoring funded by the Environmental Protection Agency, and by the National Institute of Health, for non-invasive NO and CO detection in biomedical systems by the National Institute of Health and the National Science Foundation (http://lasersci.rice.edu/).

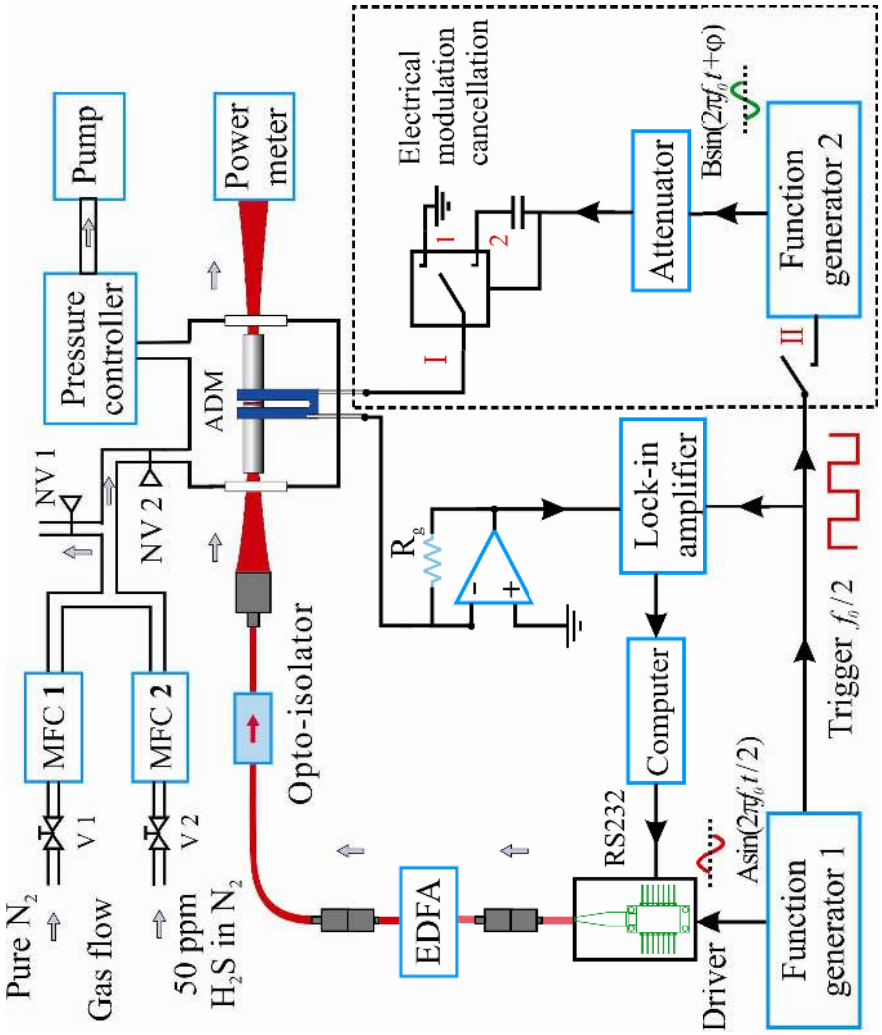
Pump
Power meter
Pressure controller
Electrical modulation cancellation
Attenuator
Function generator 2
ADM
NV 1
NV 2
MFC 1
MFC 2
V 1
V 2
Pure N_2
Gas flow
50 ppm H_2S in N_2
Opto-isolator
R_g
Lock-in amplifier
Computer
RS232
EDFA
Driver
Function generator 1
Trigger $f_0/2$
Asin($2\pi f_0 t/2$)
Bsin($2\pi f_0 t+\varphi$)
I
II
1
2

Fig. 1

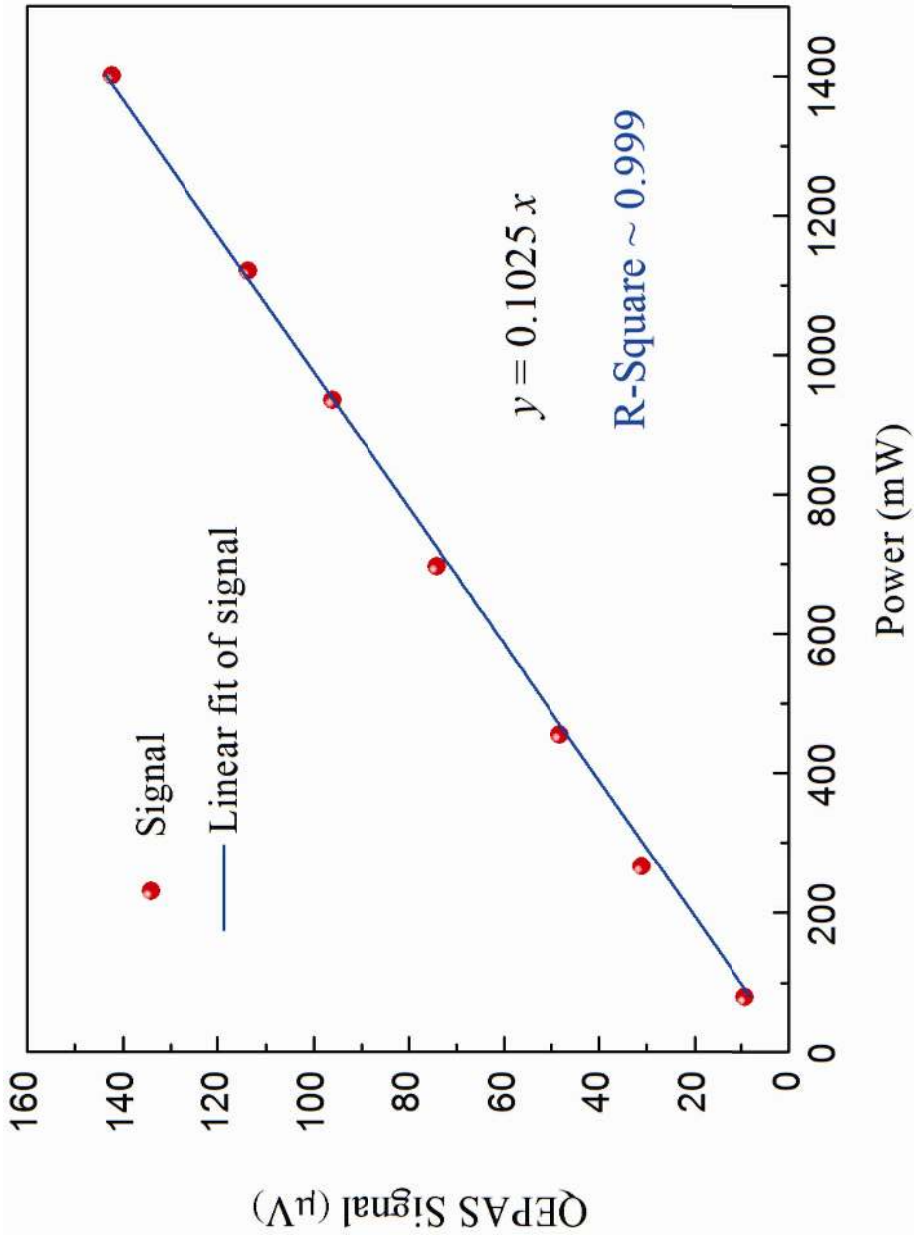
QEPAS Signal (μV)
Power (mW)
Signal
Linear fit of signal
$y = 0.1025\,x$
R-Square ~ 0.999
0
20
40
60
80
100
120
140
160
0
200
400
600
800
1000
1200
1400

Fig. 2

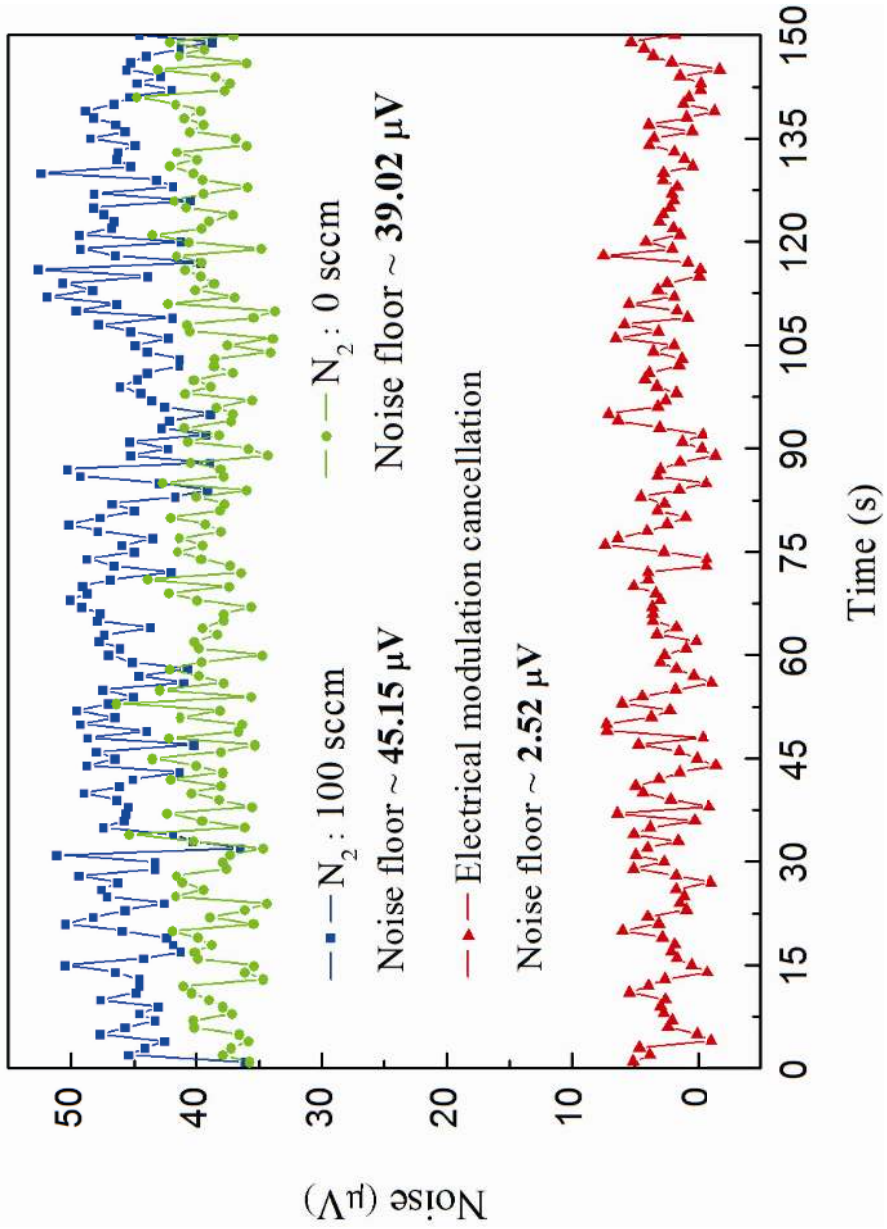
Noise (μV)
50
40
30
20
10
0
0
15
30
45
60
75
90
105
120
135
150
Time (s)
—▪— N_2 : 100 sccm
Noise floor ~ 45.15 μV
—•— N_2 : 0 sccm
Noise floor ~ 39.02 μV
—▲— Electrical modulation cancellation
Noise floor ~ 2.52 μV

Fig. 3

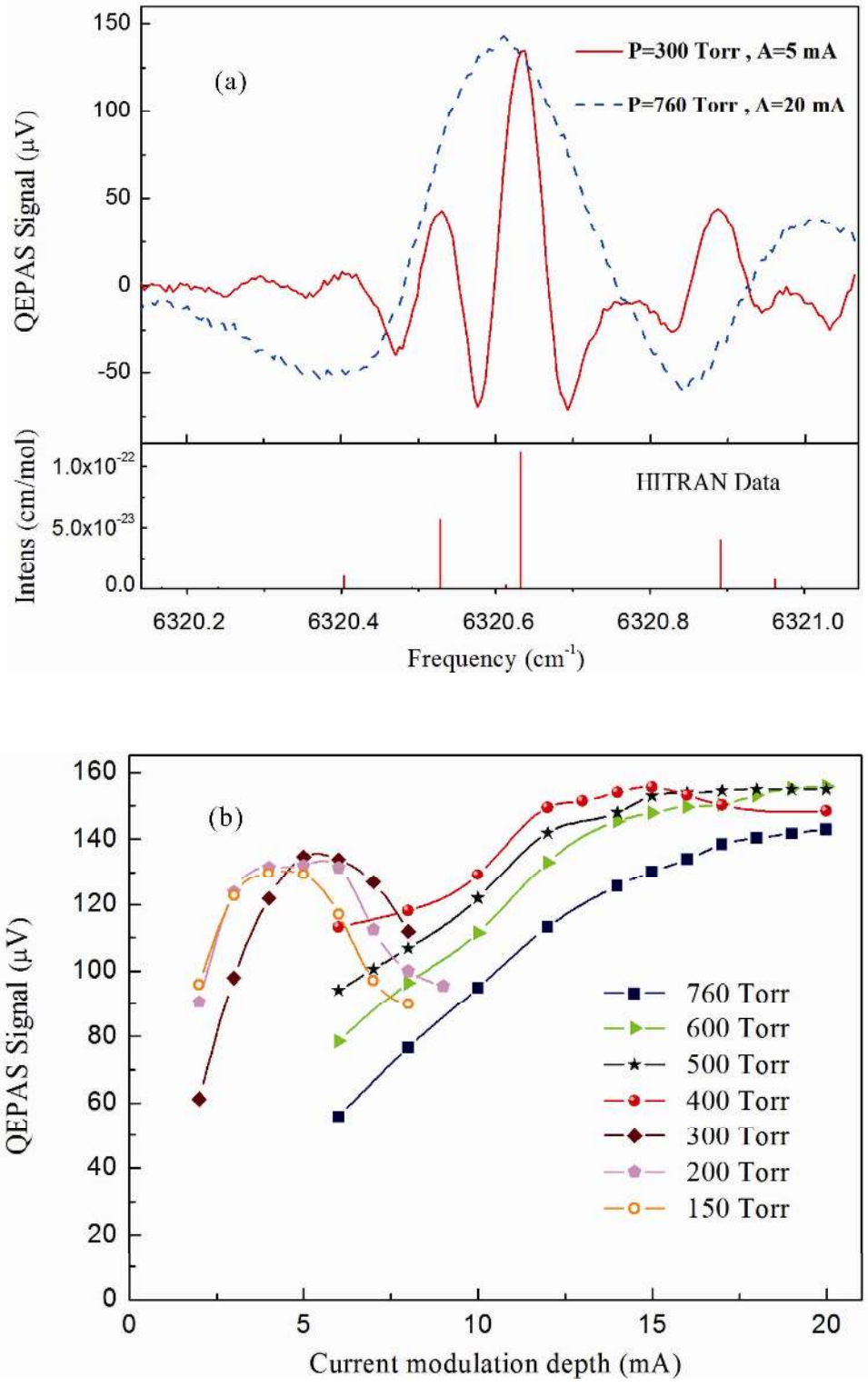
(a)
P=300 Torr , A=5 mA
P=760 Torr , A=20 mA
QEPAS Signal (μV)
150
100
50
0
-50
Intens (cm/mol)
1.0x10-22
5.0x10-23
0.0
HITRAN Data
6320.2
6320.4
6320.6
6320.8
6321.0
Frequency (cm-1)
(b)
QEPAS Signal (μV)
160
140
120
100
80
60
40
20
0
760 Torr
600 Torr
500 Torr
400 Torr
300 Torr
200 Torr
150 Torr
0
5
10
15
20
Current modulation depth (mA)

Fig. 4

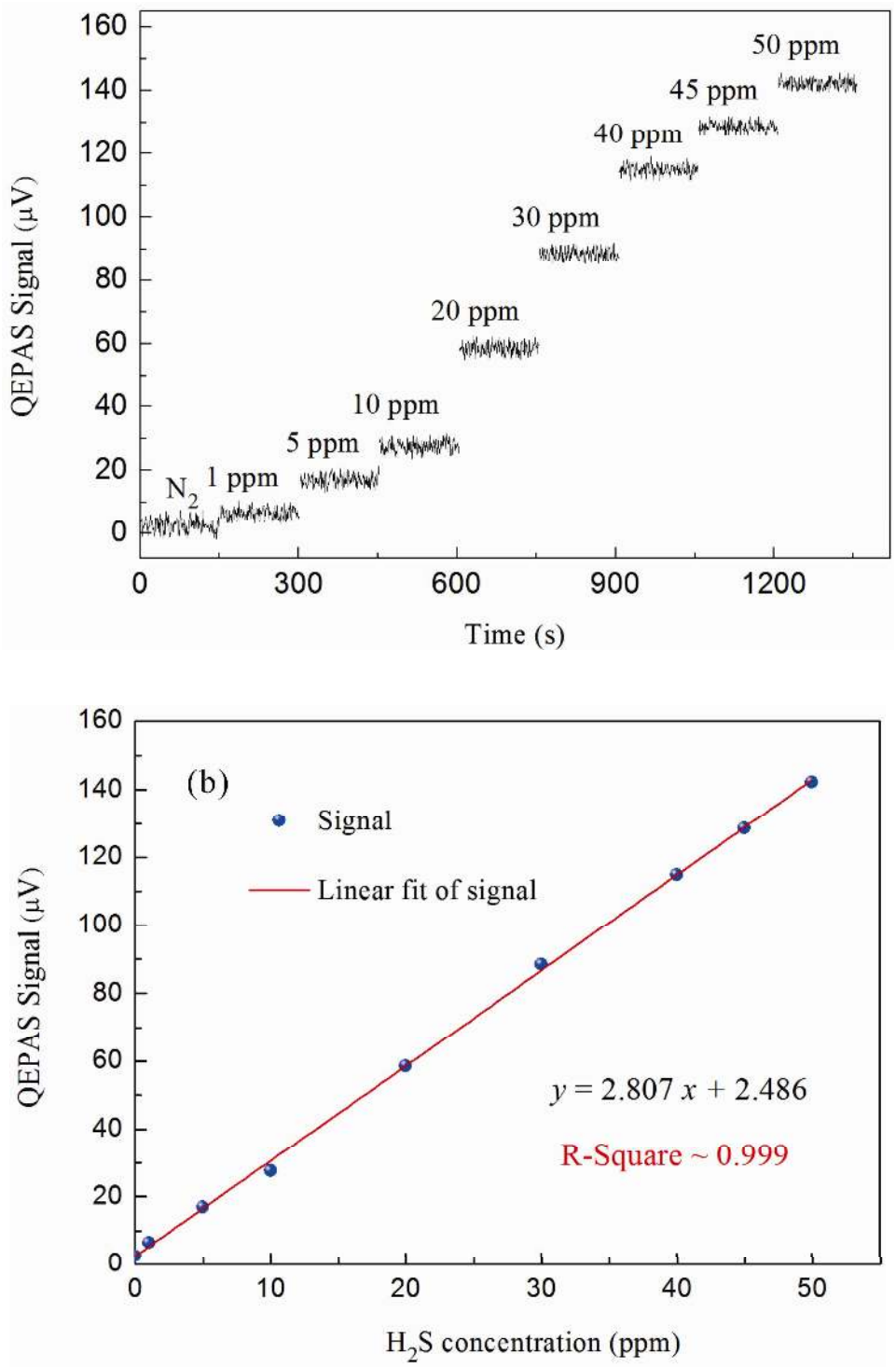
QEPAS Signal (μV)
Time (s)
N2
1 ppm
5 ppm
10 ppm
20 ppm
30 ppm
40 ppm
45 ppm
50 ppm
(b)
Signal
Linear fit of signal
y = 2.807 x + 2.486
R-Square ~ 0.999
H2S concentration (ppm)

Fig. 5

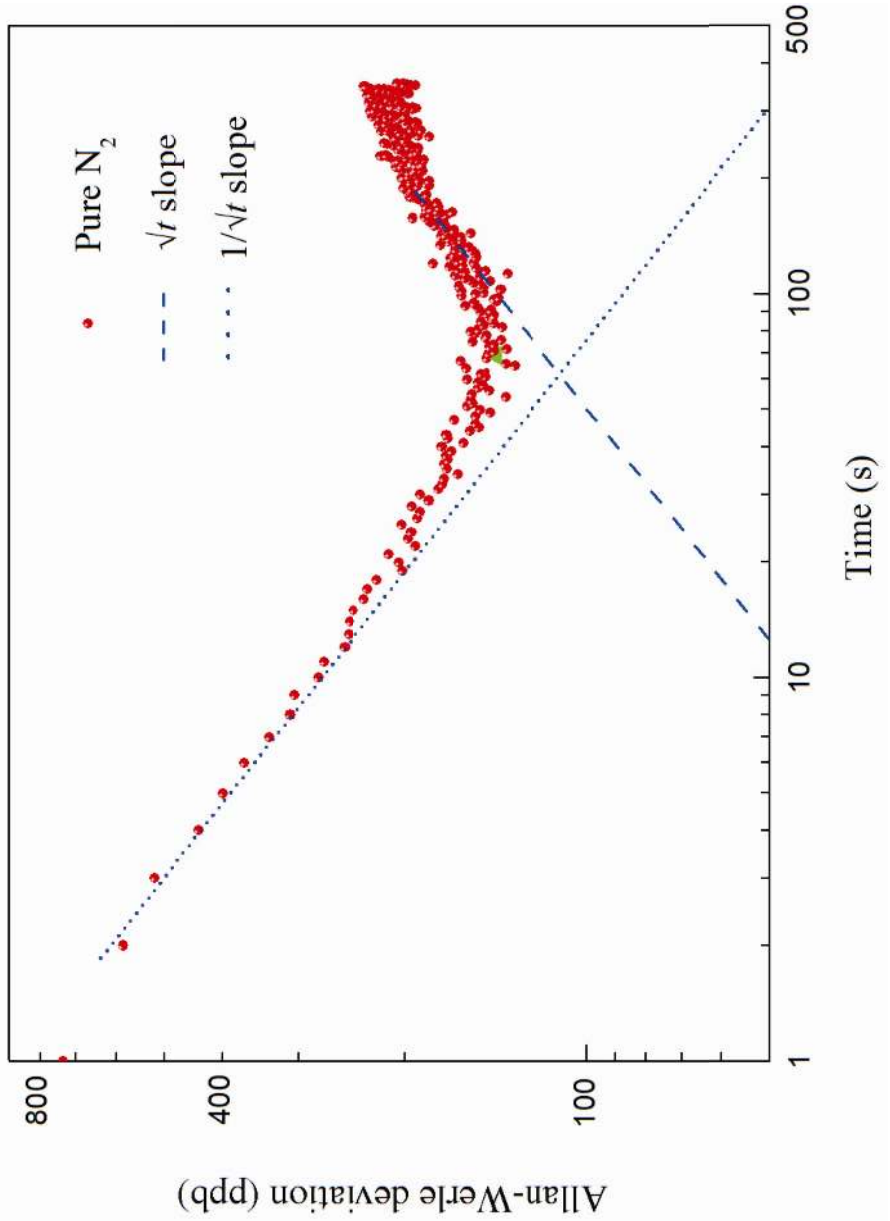
Pure N_2
$\sqrt{t}$ slope
$1/\sqrt{t}$ slope
Allan-Werle deviation (ppb)
800
400
100
1
10
100
500
Time (s)

Fig. 6